Generalization of the deflection angle in the classical scattering of particles

Daniel R. Matusek
Department of Chemistry, University of Ottawa, D'Iorio Hall, 10 Marie Curie, Ottawa, Ontario, Canada K1N 6N5
(Received 14 October 2005; published 15 March 2006)

Current conventions define the deflection angle associated with the classical elastic scattering of particles in terms of the system's position vector. This is not consistent with the definition of the scattering angle, a function of the momentum vector. A definition of the deflection angle which resolves this inconsistency is introduced and developed for the case of an arbitrary potential in two dimensions. It is shown that the generalized deflection angle reduces to that of Cross [J. Chem. Phys. **49**, 609 (1967)] when angular momentum is conserved. An efficient algorithm for the calculation of the generalized deflection angle is given and its utility in the analysis of collision dynamics is demonstrated with a numerical example.

DOI: 10.1103/PhysRevE.73.036611 PACS number(s): 45.20.−d, 45.50.Tn, 02.70.Ns

I. INTRODUCTION

Despite being one of the oldest problems in physics (dating back to the work of Newton and Huygens [1]), the classical description of scattering still finds application in modern research: astrophysics [2], electron-atom collisions [3–5], nuclear theory [6], surface [7,8] and solid-state [9] physics, and molecular collision theory (including chemical reactions) [10–13] make use of it for both qualitative and quantitative analysis. The recent discovery of chaos in scattering systems [14–16] has renewed interest in the topic and its relation to quantum mechanics via semiclassical theory [8,10,17,18]. In keeping with its importance, the treatment of central potential scattering is described in most texts on mechanics as an introduction to the topic [19,20].

The principal observable in the elastic (potential) scattering problem is the scattering angle, which measures the deviation of the system momentum from its initial orientation. This measurement forms the basis for the definition of the differential cross section [18,20,21]. When examining centrally symmetric scattering in two or three dimensions, it is common to define a deflection angle [22] which can take any value, as opposed to the scattering angle which is only defined on the principal branch (up to 180° and 360° in three and two dimensions, respectively [23]). The two angles are related and are equal for repulsive potentials; for attractive or nonmonotonic potentials, they can differ due to orbiting about the scattering center. The behavior of the deflection angle with respect to initial conditions has thus become essential to the interpretation of scattering dynamics [2,24,25].

The scattering angle is a geometric property of the system and as such it is applicable to an arbitrary potential and can be expressed in any coordinate system. However, the same cannot be said of the deflection angle. This is because there is no geometric definition of what a deflection angle is: the standard treatment of the problem is to obtain the deflection angle from the same formula used to calculate the scattering angle (in the case of repulsive potentials, e.g., Rutherford scattering) and to remark simply that the scattering angle is equal to this result modulo π (2π for two dimensions). The derivation of this "standard" formula for the two angles invokes both conservation of energy and angular momentum [19,20,22,24] and hence it is inapplicable to anisotropic or time-dependent scattering.

Within the literature a number of conventions exist regarding the above ambiguity: to use the scattering angle and make no distinction in terminology [8], or to approximate spherical symmetry and use the standard formula [5,26,27]. In contrast, the deflection angle introduced by Cross [28] is a generalization of the formula given for the standard deflection angle: here it is recognized that the integral formula for the standard deflection angle can equivalently be cast as a time integral of the angular velocity of the *position* vector. Cross's result thus gives the deflection angle in terms of the polar angle of the position long after the collision is over. If, as required by the definition of polar coordinates, the polar angle is bounded then one obtains the scattering angle from Cross's result. Contrariwise, if the polar angle θ is allowed to vary beyond its principal branch, then the deflection angle is found. This convention for the deflection angle, denoted hereinafter as $\chi_{\mathbf{r}}$, is the basis for classical scattering perturbation theory [10,29–32] and is adopted (although most often uncited) within the chaotic scattering literature [14–16,33].

There are two questions regarding Cross's definition of the deflection angle which one might ask. First, why is it a function solely of the system *position* rather than the momentum, in contradistinction to the definition of the scattering angle? Second, why is it not invariant to the choice of coordinate origin which is a property of the scattering angle? This is not to say that $\chi_{\mathbf{r}}$ is "wrong" but that its relationship to the scattering angle changes when the potential becomes noncentral. It is the purpose of the present work to provide a definition of the deflection angle which is independent of the nature of the scattering potential and of the coordinate system. Only two-dimensional scattering will be considered here as it is sufficient for the illustration of the problem.

The remainder of the present work is structured as follows: Sec. II defines the deflection angle of a two-dimensional system and examines its analytical properties; Sec. III gives results for a numerical example; Sec. IV presents concluding remarks.

II. THEORY

The deflection angle as defined by Cross is [28]

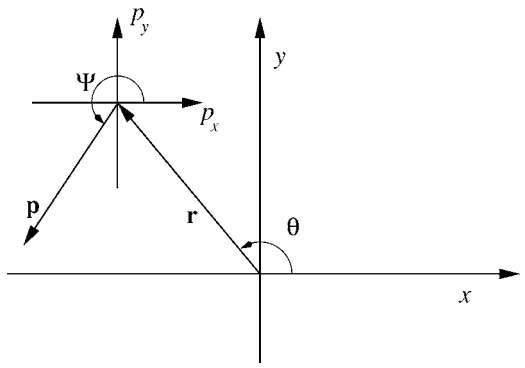

FIG. 1. Schematic diagram of a two-dimensional system. The position vector, denoted $\mathbf{r}$, has an orientation angle θ while that of the momentum vector $\mathbf{p}$ is described by the angle Ψ.

$$\chi_{\mathbf{r}} = \pi - \int_{-\infty}^{+\infty} \dot{\theta}\, dt = \pi - \theta_{+\infty}, \tag{1}$$

where $\theta_{+\infty}$ denotes the polar angle of the position $\mathbf{r}$ (see Fig. 1) long after the collision has occurred. In the case of a central potential it is straightforward to show that (1) reduces to the standard deflection angle [19]

$$\chi_{\mathbf{r}} = \pi - 2b \int_{r_0}^{\infty} \frac{dr}{r^2 \sqrt{1 - b^2/r^2 - V(r)/K}}, \tag{2}$$

where b is the impact parameter (offset from the x axis in Fig. 1), r_0 is the distance of closest approach [the largest root of the radicand in (2)], K is the initial collision kinetic energy (directed antiparallel to the x axis), and $V(r)$ is the central potential energy function of the system. Maxwell was the first to use this result (generalized from celestial mechanics) to examine scattering of r^{-n} potentials in connection with the kinetic theory of gases [34,35]; in this instance, as in that of Rutherford scattering, (2) yields the scattering angle. The first calculation of a deflection angle from (2) appears to be Hirschfelder's [36] where the Lennard-Jones (6,12) potential was used.

As mentioned in the introduction, if $\theta_{+\infty} \in [0, 2\pi)$, then $\chi_{\mathbf{r}}$ is equal to the scattering angle. This is consistent with the definition of an angle in a polar coordinate system (see Fig. 1): the representation of an arbitrary $\mathbf{r}$ must be unique and hence $\theta = \arctan(y/x)$, where (x, y) are the Cartesian components of the position vector. However, θ can also be expressed as a canonical coordinate and one can obtain $|\theta| \geqslant 2\pi$ from solving the equations of motion for the system. Doing so is equivalent to redefining $\theta = \mathrm{Arctan}(y/x)$, which is a multivalued function (the notation of Abramowitz and Stegun is adopted for the inverse trigonometric functions [37]). Whatever the manner of its determination, the key to the definition of $\chi_{\mathbf{r}}$ is the generalization of θ to become a multivalued function.

By allowing the orientation angle of the position vector to become a multivalued function, the deflection angle can be calculated for a central potential. However, what is implicit in the standard definition, and lacking in any other convention currently in use, is that the deflection angle is the multivalued generalization of the scattering angle. Adopting this definition is consistent with that of the scattering angle in that it is defined solely in terms of the momentum vector and is independent of the choice of coordinate system. To define a deflection angle related to $\mathbf{p}$, let Ψ be the polar angle which describes the orientation of $\mathbf{p}$ (see Fig. 1). It is in principle possible to generalize $\Psi(t)$ to be a multivalued function and not restricted to the principal branch. Therefore the generalized deflection angle for two-dimensional motion $\chi_{\mathbf{p}}$ is defined as

$$\chi_{\mathbf{p}} = \Psi_{-\infty} - \Psi_{+\infty}. \tag{3}$$

Using the usual Cartesian-polar relationships, $\Psi(t)$ may be represented as

$$\Psi(t) = \mathrm{Arctan}\left(\frac{p_y}{p_x}\right) \equiv \arctan\left(\frac{p_y}{p_x}\right) + k_\Psi \pi, \tag{4}$$

where k_Ψ is an integer which determines the branch of Ψ. The Cartesian momenta p_x and p_y are along and perpendicular to the principal axis, respectively (see Fig. 1).

In order to examine the correspondence with $\chi_{\mathbf{r}}$, the Cartesian momenta components are transformed to those conjugate to the polar representation of $\mathbf{r}$: $p_x = p_r \cos\theta - (p_\theta/r)\sin\theta$ and $p_y = p_r \sin\theta + (p_\theta/r)\cos\theta$. Substitution of this and letting

$$\gamma = \mathrm{Arctan}\left(\frac{p_\theta}{r p_r}\right) \tag{5}$$

gives

$$\Psi = \theta + \gamma \equiv \theta + \gamma_0 + k_\gamma \pi. \tag{6}$$

Here $\gamma_0 \equiv \arctan(p_\theta/r p_r) \in [-\pi/2, +\pi/2]$, and k_γ is an integer that determines the branch of γ.[1] The branch of the polar angle of $\mathbf{r}$ is implied since it is assumed to also be a multivalued function. Evaluation of $\Psi(t)$ as $t \to \pm\infty$ is accomplished by noting that in both limits $r \to \infty$. This gives from (5) that

$$\lim_{t \to \pm\infty} \tan\gamma = 0, \tag{7}$$

and hence $\gamma_0 \to 0$. Substitution of the above result into (6) and (3) gives

$$\chi_{\mathbf{p}} = (k_{\gamma,-\infty} - k_{\gamma,+\infty})\pi + \theta_{-\infty} - \theta_{+\infty}. \tag{8}$$

The problem of determining $\chi_{\mathbf{p}}$ is reduced to the determination of $k_{\gamma,\pm\infty}$ and $\theta_{+\infty}$.

As γ is a function of the canonical variables, it is a continuous function of time inasmuch as the system is itself. The integer k_γ is necessarily a discontinuous function which changes every time that $\gamma(t)$ crosses the branch cut of the arctan function (this is the p_y axis of Fig. 1 for the current choice of branch cut). Thus $k_\gamma(t)$ changes only for a discrete set of events $t_i \in T$,

[1] The particular choice of the principal branch for arctan does not affect the overall result of Ψ. It does, however, affect the definition of $a_\gamma(T_C)$ and analogous quantities; hence, $\arctan(f) \in [-\pi/2, +\pi/2]$ is used throughout for consistency.

$$k_\gamma = \sum_{t_i \in T} a_\gamma(T) u(t - t_i), \tag{9}$$

where $u(x)$ is a unit step function and $T \equiv T_C \cup T_D$ denotes the set of events when γ changes branch through continuous and discontinuous motion, respectively; the integer coefficients $a_\gamma(T)$ are dependent on the type of event T. Note that all subsequent quantities that are labeled with the subscript i imply $t=t_i$ or $t \to t_i^-$ where the limits are different. Similarly, all quantities labeled with a $\pm$ superscript denote evaluation at $t=t_i \pm \epsilon$, with $\epsilon > 0$.

To find $t_i \in T_C$ and the corresponding $\{a_\gamma(T_C)\}$, consider the behavior of $\gamma(t)$ near such an event: assuming that $\gamma(t)$ is continuous as $t \to t_i$, then $\dot{\gamma} = \dot{\gamma}_0$. For γ to change branch it must approach the limit $\gamma_0 \pm \pi/2$ and have a nonzero time derivative with the same sign. However, $\gamma_0(t)$ has a discontinuity at this point; hence k_γ must be adjusted to enforce the continuity of $\gamma(t)$ at t_i. More formally, this is summarized as (see footnote 1).

$$T_C \equiv \{t_i | \gamma_{0,i} = \pm \pi/2,\ \dot{\gamma}_{0,i} \neq 0,\ \mathrm{sgn}(\dot{\gamma}_{0,i}) = \mathrm{sgn}(\gamma_{0,i})\}. \tag{10}$$

The final condition of T_C excludes the case of $\gamma_0(t)$ passing through a local extremum.

The values of the $a_\gamma(T_C)$ are found from the condition of continuity:

$$\lim_{t \to t_i^-} \gamma(t) = \lim_{t \to t_i^+} \gamma(t), \tag{11}$$

and noting that

$$\lim_{t \to t_i^+} \gamma_0(t) = -\gamma_{0,i}, \tag{12}$$

which is a basic property of the arctan function. By definition $k_\gamma^+ = k_\gamma^- + a_\gamma(T_C)$; using this with (12) in (11) gives

$$a_\gamma(T_C) = \mathrm{sgn}(\gamma_{0,i}). \tag{13}$$

The results of (10) and (13) are not dependent on the choice of coordinate system although (10) will have a different representation for different choices.

The set of discontinuous events T_D which occur depend on the Hamiltonian of the system and on the behavior of γ_0 near the origin of both $\mathbf{r}$ and $\mathbf{p}$. The subsets of T_D events are

$$T_D = T_I \cup T_R \cup T_0, \tag{14}$$

where T_I denote the set of events where impulsive forces occur, T_R where $\mathbf{p}$ is inverted, and T_0 the instances where the system passes through the coordinate origin. The coefficients $\{a_\gamma(T_I)\}$ of impulsive events can be expressed directly as (generally noninteger) changes to both $|\mathbf{p}|$ and Ψ; however, the event times T_I have no general formulation since they may contain both time- and coordinate-dependent conditions (e.g., moving hard disk collisions). Therefore T_I will not be treated explicitly here.

The case of the momentum being inverted occurs when $\mathbf{p}$ passes through zero smoothly or otherwise, the latter being a T_I event. From (5), it appears that γ_0 and $\dot{\gamma}_0$ are undefined but both do in fact possess well-defined limits under such conditions:

$$\gamma_{0,i} = \arctan\left(\frac{\dot{p}_{\theta,i}}{r_i \dot{p}_{r,i}}\right), \tag{15a}$$

$$\dot{\gamma}_{0,i} = \lim_{t \to t_i^-} \frac{r p_r \dot{p}_\theta - \mu^{-1} p_r^2 p_\theta - r \dot{p}_r p_\theta}{r^2 p_r^2 + p_\theta^2} \tag{15b}$$

$$= \frac{r \dot{p}_r \ddot{p}_\theta - r \dot{p}_\theta \ddot{p}_r}{2(r^2 \dot{p}_r^2 + \dot{p}_\theta^2)}. \tag{15c}$$

Here μ denotes the reduced mass of the system. It should be noted that $\dot{\gamma}_{0,i}$ is zero unless the potential is explicitly dependent on time. Hence the change associated with Ψ when $\mathbf{p}$ is inverted is not brought about by continuous change in γ_0. To account for the change in orientation of the momentum vector, a correction must be applied to γ. Formally the correction is derived from the conditions of inversion for $\mathbf{p}$:

$$p_r = |\mathbf{p}| \cos \gamma, \tag{16a}$$

$$p_\theta = r |\mathbf{p}| \sin \gamma, \tag{16b}$$

and $p_j^+ = -p_j^-$ with $j \in \{r, \theta\}$. Consideration of (16) shows that for both components to change sign, γ must be shifted by an odd multiple of π. The particular integer is chosen by convention to be -1; this choice yields a deflection angle of π for a head-on collision [$\theta_{+\infty} = 0$ in (1)] and thus maintains consistency with the standard deflection angle [19]. Therefore

$$a_\gamma(T_R) = -1, \tag{17}$$

where the T_R events describe the conditions for a nonimpulsive inversion of $\mathbf{p}$,

$$T_R \equiv \{t_i | \mathbf{p}_i = \mathbf{0},\ \dot{\mathbf{p}}_i \neq \mathbf{0}\}, \tag{18}$$

and $\mathbf{0}$ denotes the zero vector. Note that (18) is defined without any reference to a particular coordinate system.

The final correction that must be applied to γ occurs when the system passes through the coordinate origin, denoted by the set of events T_0. The conditions for this are similar to those of T_R but applied to $\mathbf{r}$:

$$T_0 \equiv \{t_i | \mathbf{r}_i = \mathbf{0},\ \dot{\mathbf{r}}_i \neq \mathbf{0}\}. \tag{19}$$

Note that from (16) the condition $p_{\theta,i} = 0$ is implied in (19). The inversion of $\mathbf{r}$ requires that θ be shifted by an odd multiple of π and the value of

$$a_\theta(T_0) = 1 \tag{20}$$

is chosen to maintain agreement with (1) for rectilinear motion which passes through the origin. In this case, $\theta_{+\infty} = \pi$ and hence $\chi_{\mathbf{r}} = 0$. It follows from this choice that in order for $\chi_{\mathbf{p}}$ to also be zero for such motion, Ψ must be unchanged by a T_0 event. Thus (20) requires that γ be shifted by an equal and opposite amount,

$$a_\gamma(T_0) = -1. \tag{21}$$

Once the set of events T has been determined for a particular trajectory, the deflection angle can be evaluated from (8). The Appendix describes an algorithm to determine T_C, T_0, and T_R events by bracketing the zeros of the momentum components. In order to examine the basic properties of $\chi_{\mathbf{p}}$ it is sufficient to know that in principle T can be found.

Some basic results can be derived about $\chi_{\mathbf{p}}$ from (16). First, consider the definition of a scattering trajectory, i.e., $p_{r,\pm\infty} \gtrless 0$,

$$\frac{p_{r,+\infty}p_{r,-\infty}}{|\mathbf{p}_{+\infty}||\mathbf{p}_{-\infty}|} = \cos\gamma_{+\infty}\cos\gamma_{-\infty} = (-1)^{k_{\gamma,+\infty}+k_{\gamma,-\infty}} = -1, \tag{22}$$

which is obtained from (16) and (7). The conclusion of (22) is

$$k_{\gamma,-\infty} + k_{\gamma,+\infty} = 2m - 1, \quad m \in \mathbb{Z}, \tag{23}$$

which places a restriction on the sequence of allowable events in T. A corollary of (23) is the relation between $\chi_{\mathbf{p}}$ and $\chi_{\mathbf{r}}$ [using (1) and (8)]:

$$\chi_{\mathbf{p}} - \chi_{\mathbf{r}} = 2(k_{\gamma,-\infty} - m)\pi. \tag{24}$$

Here, the special case of $\theta_{-\infty}=0$ was used in $\chi_{\mathbf{p}}$ for the sake of comparison. The meaning of (24) is that, while $\chi_{\mathbf{r}}$ contains information on the loops about the coordinate origin, $\chi_{\mathbf{p}}$ contains additional information on the loops about points *other* than the origin. It should also be noted that because of (24) the two angles will yield identical scattering angle functions and hence either may be used to obtain the classical cross section.

Finally, the conditions where $\chi_{\mathbf{p}}$ and $\chi_{\mathbf{r}}$ are equal can be found by considering a type of symbolic dynamics. Any trajectory has a sequence of events $t_i \in T$ associated with it (although this does not distinguish it uniquely in general). When angular momentum is conserved, $(T_R \cup T_0) \cap T = \varnothing$ since T_R would violate the hypothesis and T_0 only occur for the trivial case of $p_\theta = 0$. From (A2), T_C events differ by the sign of $\dot{p}_{r,i}$ when p_θ is constant; let $T_C^{\pm}$ denote events corresponding to $\mathrm{sgn}\dot{p}_{r,i} = \pm 1$. Since p_r is initially negative it follows that any trajectory which conserves angular momentum has a sequence $T_C^+ T_C^- T_C^+ \cdots T_C^+$, where the final event must be T_C^+ for the trajectory to escape the region of interaction. Thus associated series of $a_\gamma(T_C)$ for such a trajectory is

$$a_\gamma(T_C^+) + a_\gamma(T_C^-) + \cdots + a_\gamma(T_C^+) = (n+1)a_\gamma(T_C^+) + n a_\gamma(T_C^-) = -\mathrm{sgn}\, p_\theta, \tag{25}$$

where in the last line (A1) of the Appendix has been used. Therefore substitution into (9) gives

$$\chi_{\mathbf{p}} = \pi\, \mathrm{sgn}\, p_\theta - \theta_{+\infty} + \theta_{-\infty} \tag{26}$$

for a trajectory that conserves angular momentum. To compare with (1), $\theta_{-\infty}=0$ and $p_\theta > 0$ are required, and (26) shows that $\chi_{\mathbf{p}} = \chi_{\mathbf{r}}$. The case of a central potential is described by (25) where $n=0$. Cases of correspondence similar to (26) could be derived once the set of allowed events in T are specified, i.e., $m \neq 0$ but constant in (24). Such analysis could be fruitful in the case where potential or dynamical symmetries restrict the allowed events in T.

III. NUMERICAL EXAMPLE

Since both $\chi_{\mathbf{r}}$ and $\chi_{\mathbf{p}}$ generate identical differential cross sections, it is necessary to demonstrate that $\chi_{\mathbf{p}}$ is useful in the analysis of dynamical systems. An exemplary system for this purpose is that of two-dimensional potential scattering by an off-centered central potential. The Hamiltonian of this system is

$$H = \frac{1}{2}\left(p_r^2 + \frac{p_\theta^2}{r^2}\right) + R^{-6}(R^{-6} - 2), \tag{27}$$

where

$$R(r,\theta) = \sqrt{(r\cos\theta - x_c)^2 + (r\sin\theta - y_c)^2}, \tag{28}$$

and (x_c, y_c) are the Cartesian coordinates for the center of force. Note that the reduced mass is taken as unity without any loss of generality and indeed the units chosen are arbitrary since they may be scaled to produce a Hamiltonian identical to (27). The numerical solution to the resulting equations of motion for a given set of initial conditions (b,K) is straightforward and in this particular example was performed using the algorithm of Bulirsch and Stoer [38,39]. The initial velocity was antiparallel to the x axis, and all trajectories started and finished at $r \geqslant 100$.

The Hamiltonian (27) describes a Lennard-Jones (6,12) potential whose origin is offset from that of the coordinate system. When the center of force is coincident with the coordinate origin, the resulting deflection function is well documented [24,25,36,40]: starting from a maximum value of π at the head-on collision ($b=0$), $\chi_{\mathbf{r}}(b)$ decreases to a negative, finite (infinite) minimum for K above (below) a critical energy. After passing through the minimum, $\chi_{\mathbf{r}}(b)$ asymptotically approaches zero for large b. Such behavior is generic to all reasonable potential energy forms [25].

When $(x_c, y_c) \neq \mathbf{0}$, $\chi_{\mathbf{r}}$ ceases to reproduce the correct behavior as is seen from Fig. 2(a). Here $\chi_{\mathbf{r}}$ vs b is shown for $(x_c, y_c) = (0, 10)$ and $K = 0.1$, which is below the critical energy. The orbiting singularities manifest themselves as regions of irregular oscillations for $b \approx 8$ and $b \approx 12$. The head-on collision at $b=10$ yields a deflection of π as expected and $\chi_{\mathbf{r}}$ approaches zero asymptotically but beyond this there is little that is indicative of the underlying dynamics. In particular, the symmetry of $\chi_{\mathbf{r}}$ about the head-on collision is not observed as it is in the case of $(x_c, y_c) = \mathbf{0}$ (not shown) which is $\chi_{\mathbf{r}}(-b) = 2\pi - \chi_{\mathbf{r}}(b)$.

In contrast to the behavior of $\chi_{\mathbf{r}}$, the deflection function of $\chi_{\mathbf{p}}$ shown in Fig. 2(b) is an exact reproduction of the literature results for the Lennard-Jones potential when $b > 10$, including the orbiting singularity [25,36]. The behavior for $b < 10$ shows that $\chi_{\mathbf{p}}$ has odd symmetry with respect to the impact parameter. This symmetry is to be expected from consideration of the $(x_c, y_c) = \mathbf{0}$ system. The potential is symmetric with respect to reflection about the x axis and hence trajectories with $b < 0$ will be related to those of $b > 0$ in the same way. Thus the variation of θ over the path is an odd

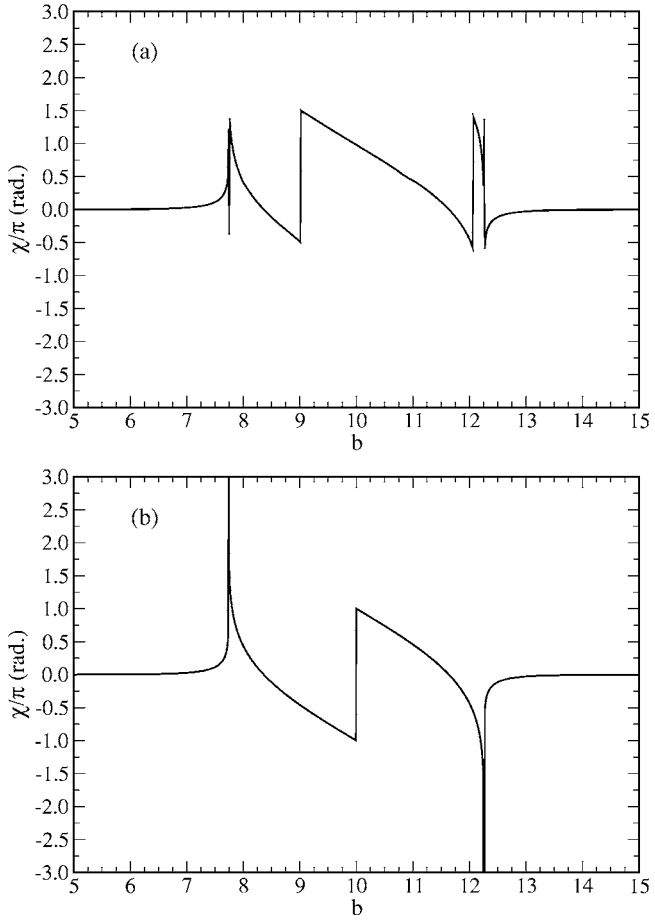

FIG. 2. The deflection functions for (27) with $K=0.1$ and $(x_c,y_c)=(0,10)$. (a) $\chi_{\mathbf{r}}$ vs b; (b) $\chi_{\mathbf{p}}$ vs b.

function of impact parameter [2]. Similarly, γ is also an odd function of b as it is dependent on the angular momentum [from (5) and $p_\theta=b\sqrt{2K}$]. Hence, $\Psi(b)$ is odd. In the off-centered potential $\chi_{\mathbf{p}}$ still has the same symmetry as it is not dependent on the choice of origin.

That $\chi_{\mathbf{p}}$ possesses the symmetry properties of the trajectories, and hence the Hamiltonian, while $\chi_{\mathbf{r}}$ does not, is an important point to note as this aids in the interpretation of the dynamics of the system. At first glance the behavior of $\chi_{\mathbf{r}}(b)$ in Fig. 2(a) implies a complex dynamics and would require further analysis of other observables (e.g., time delay) to reveal its underlying simplicity.

IV. SUMMARY AND REMARKS

It has been shown that current conventions regarding the deflection angle in classical particle scattering are not generalizations of the expression valid for a central potential. A deflection angle is a multivalued generalization of the corresponding scattering angle, and hence is based on the properties of the momentum vector. The current usages of deflection angles are based on the properties of the position vector and, while being formally inconsistent, also suffer from lack of invariance to the choice of origin. The generalization of the deflection angle based on the momentum vector was given, along with an algorithm for its calculation, and its representation in polar coordinates. The elementary analytical properties of $\chi_{\mathbf{p}}$ were also derived, showing that $\chi_{\mathbf{p}}$ and $\chi_{\mathbf{r}}$ will always differ by a multiple of 2π and are equal when angular momentum is conserved. Finally, a simple numerical example was given which showed that $\chi_{\mathbf{p}}$ can describe orbiting about points not coincident with the origin and reflects the symmetries of the system in a simple way.

The implications of this work are threefold. First, dynamical systems can be analyzed more efficiently by use of $\chi_{\mathbf{p}}$ especially in conjunction with $\chi_{\mathbf{r}}$ as this would separate partially the contributions to the motion. In particular, use of $\chi_{\mathbf{p}}$ may show that the underlying dynamics are more "regular" than what would be inferred from $\chi_{\mathbf{r}}$.

Second, there now exists a means to treat scattering of an arbitrary number of bodies with arbitrary interaction. While only an (effectively) one-body problem was considered here, the definition of $\chi_{\mathbf{p}}$ applies to each member of a many-body system, i.e., $\chi_{\mathbf{p},n}$ for every n in an ensemble (these will of course be related kinematically).

Finally, $\chi_{\mathbf{p}}$ represents an alternative basis for calculating the differential cross section; although use of $\chi_{\mathbf{p}}$ or $\chi_{\mathbf{r}}$ formally yields identical results (since they all differ by multiples of 2π), numerical difficulties may recommend one over the other. For example, Figs. 2(a) and 2(b) will have different differential cross sections if the deflection functions are splined and then used to obtain the scattering angle as a function of impact parameter. This is because the orbiting of the system results in finite oscillations in $\chi_{\mathbf{r}}$ which may lead to false rainbow angles in the differential cross section. In $\chi_{\mathbf{p}}$, orbiting manifests itself as a singularity, which is known to have an exponential decay contribution to the differential cross section [25,40]. Such numerical difficulties may explain some of the findings in the literature [16,41].

The present work only considers two dimensions. Similar results obtained for three-dimensional scattering are being prepared for a future publication.

APPENDIX: ALGORITHM FOR k_γ

In order to make practical use of (8), $k_\gamma(t)$ must be found. It is assumed that the equations of motion for the system are solved in polar coordinates (r,θ) so that $\theta_{\pm\infty}$ are known. The set of relevant events is $T=T_C\cup T_0\cup T_R$ (a smooth potential is assumed, hence T_I are excluded). Since the information about the trajectory is expressed in (r,θ,p_r,p_θ), the definition of the events should be reexpressed in terms of this choice of coordinates. Thus for T_C, $\gamma_{0,i}=\pm\pi/2$ translates to $p_{r,i}=0$ with $p_{\theta,i}\neq 0$ by (5). Substitution of these conditions into the formula for $\dot{\gamma}_0$ (15) gives $\dot{\gamma}\neq 0\Rightarrow\dot{p}_{r,i}\neq 0$. Thus

$$T_C=\{t_i|p_{r,i}=0,\ p_{\theta,i}\neq 0,\ \dot{p}_{r,i}\neq 0\}. \tag{A1}$$

The expression for $a_\gamma(T_C)$ in polar coordinates is found by using $\mathrm{sgn}(\gamma_{0,i})=\mathrm{sgn}(\tan\gamma_{0,i})$ in (13) as this is true when the conditions (A1) are satisfied; substitution of $p_{r,i}^-=-\epsilon\dot{p}_{r,i}$ in this yields the final result

TABLE I. Possible combinations of $\sigma_r^{\pm}$ and their associated actions required to bracket T_0 events. The table entries refer to the possible values of $\{-1,0,+1\}$ for $\sigma_r^{\pm}$.

σ_r^-	σ_r^+	A_i[a]	σ_r^-	σ_r^+	A_i[a]	σ_r^-	σ_r^+	A_i[a]
+	+		0	+	A_2	−	+	
+	0	A_0	0	0		−	0	
+	−	A_1	0	−	A_2	−	−	

[a]Actions: A_0, store σ_r^- in s; A_1, $t_i \in T_0$ bracketed, apply $a_\theta(T_0)=+1$, $a_\gamma(T_0)=-1$; A_2, reevaluate table lookup with (s,σ_r^+).

$$a_\gamma(T_C) = \lim_{t\to t_i^-} \operatorname{sgn}(\gamma_0) = -\operatorname{sgn}(p_{\theta,i})\operatorname{sgn}(\dot{p}_{r,i}), \tag{A2}$$

where it has been assumed that $r>0$ throughout.

In terms of a polar coordinate system, the definition of T_R events (18) becomes

$$\begin{aligned} T_R = &\{t_i | p_{r,i}=0, p_{\theta,i}=0, \dot{p}_{r,i}=0, \dot{p}_{\theta,i}\neq 0\} \\ &\cup \{t_i | p_{r,i}=0, p_{\theta,i}=0, \dot{p}_{r,i}\neq 0, \dot{p}_{\theta,i}=0\} \\ &\cup \{t_i | p_{r,i}=0, p_{\theta,i}=0, \dot{p}_{r,i}\neq 0, \dot{p}_{\theta,i}\neq 0\}. \end{aligned} \tag{A3}$$

As per (17), the correction coefficient is still -1.

The set of events T_0 can be identified using $r=|\mathbf{r}|$ and its conjugate momentum in the formal definition of (19):

$$T_0 = \{t_i | r_i = 0, p_{r,i} \neq 0\}. \tag{A4}$$

Note that $p_{\theta,i}=0$ is a necessary condition of (A4). Although the algorithm presented here is supposed to calculate k_γ, the correction factor (20) is required for θ in addition to (21). Furthermore, corrections will have to be applied to r and p_r to ensure that their behavior is correct in passing through the origin (this is not necessarily ensured by the integrator). Specifically, p_r must change sign to reflect the fact that the system moves away from the origin and $r \geqslant 0$ must be enforced.

From (A1), (A3), and (A4), it is clear that events can be determined by finding the roots of $p_r(t)=0$ and $p_\theta(t)=0$. Therefore, the basic means of locating $t_i \in T$ is that of root bracketing [38]. If $f(t)$ is one of the canonical coordinates or momenta then for any time t let

$$\sigma_f^{\pm} = \begin{cases} \operatorname{sgn} f(t \pm \epsilon), & |f| \neq 0, \\ 0, & |f| = 0. \end{cases} \tag{A5}$$

Here $\epsilon>0$ is a small time interval such that f is monotonic on $[t-\epsilon, t+\epsilon]$. Bracketing works by dividing the trajectory into time segments of 2ϵ and noting changes in the sign of σ_f. If ϵ is small enough that only one root $f=0$ is bracketed on a segment, only the current point in time σ_f^+ and the one immediately preceding it σ_f^-, need be known. The combinations of (σ_f^-, σ_f^+) can be used as indices for a lookup table function which gives instructions on what event has occurred.

For $t_i \in T_0$, only $\sigma_r^{\pm}$ are needed to track a sign change in r. The nine possible combinations of (σ_r^-, σ_r^+) are shown in Table I along with their associated actions $\{A_i\}$. The first thing to note about Table I is that the combinations of r going from negative to positive values will not occur since any corrections will immediately map r to positive values. When a change in sign is detected [e.g., the $(+,-)$ entry], the associated action A_1 requires that the corrections be applied to both θ and γ to preserve the value of Ψ; moreover, both r and p_r must be mapped to positive values since this is required by the definition of the polar coordinate system and (16). The ambiguous cases occur when $r=0$: whether such a point is part of a T_0 event or r passing through a minimum depends on the subsequent time step. The solution in this case is storing $s \leftarrow \sigma_r^- \neq 0$ upon the first occurrence of $\sigma_r^+ = 0$ (action A_0) and recalling it when σ_r^+ first becomes nonzero again (action A_2). Evaluating the sequence (s, σ_r^+) using the same table entries ensures that the time interval is widened enough to bracket the root of $r(t)=0$. The algorithm to bracket T_0 events is therefore

(1) evaluate σ_r^+ for the current time step,
(2) find A_i from Table I using (σ_r^-, σ_r^+),
(3) update $(r, \theta, p_r, k_\gamma)$ according to the A_i,
(4) store $\sigma_r^- \leftarrow \sigma_r^+$ for the next time step.

An approach similar to the above is adopted for bracketing T_C and T_R events. Since both T_C and T_R require $p_{r,i}=0$, the behavior of p_θ is what differentiates them. Hence the possible combinations of $(\sigma_{p_r}^-, \sigma_{p_r}^+, \sigma_{p_\theta}^-, \sigma_{p_\theta}^+)$ are used to define the lookup table function, the results of which are given in Table II. The entries in Table II are the type of event E and the associated action A for a given $(\sigma_{p_r}^-, \sigma_{p_r}^+, \sigma_{p_\theta}^-, \sigma_{p_\theta}^+)$. The types of events are T_C, T_R, ambiguous X, and nonevents $\varnothing$. Actions associated with T_C and T_R events are the appropriate values of $a_\gamma(T)$ (nonevents, of course, do not require a correction). Ambiguous events have the actions J_i associated with them.

To derive the appropriate $\{A_i\}$ for Table II, the following assumptions have been made. First, $\epsilon>0$ is small enough that if one of the $\sigma_f^{\pm}$ are zero, then $f(t)$ is nonzero over the rest of the interval [e.g., the $(+,-,0,-)$ entry of Table II]. Second, if σ_f^- is zero then, in a time interval centered around this point, $g(t)$ (the other momentum component) can be taken as being constant on such a shifted interval (this is true for a small enough ϵ); examples of such a case are found in the $(0,0,0,+)$ and $(0,+,-,+)$ entries of Table II. Finally, the value of $a_\gamma(T_C)$ can be calculated from (A2) using $(\sigma_{p_r}^-, \sigma_{p_r}^+, \sigma_{p_\theta}^-, \sigma_{p_\theta}^+)$:

$$a_\gamma(T_C) = \frac{1}{4}(\sigma_{p_r}^- - \sigma_{p_r}^+)(\sigma_{p_\theta}^- + \sigma_{p_\theta}^+), \tag{A6}$$

where the sign of $\operatorname{sgn}(\dot{p}_{r,i})$ is found from the approximation $\dot{p}_{r,i} = (p_{r,i}^+ - p_{r,i}^-)/2\epsilon$.

The first few $\{J_i\}$ $(i=1,2,3)$ are concerned with the first occurrence of a zero in one or both of the σ^+ as this requires the storage of the last nonzero σ^-. Actions J_4 and J_5 are required when a T_C event is bracketed *and* a zero in p_θ is encountered. Actions J_6 and J_7 occur when p_r becomes nonzero again: s_r is substituted for $\sigma_{p_r}^-$ and the new string $(s_r, \sigma_{p_r}^+, \sigma_{p_\theta}^-, \sigma_{p_\theta}^-)$ is used for evaluating the interval. The

TABLE II. Bracketing T_C and T_R events from $(\sigma^-_{p_r}, \sigma^+_{p_r}, \sigma^-_{p_\theta}, \sigma^+_{p_\theta})$.

$\sigma^-_{p_r}$	$\sigma^+_{p_r}$	$\sigma^-_{p_\theta}$	$\sigma^+_{p_\theta}$	E^a	A^b	$\sigma^-_{p_r}$	$\sigma^+_{p_r}$	$\sigma^-_{p_\theta}$	$\sigma^+_{p_\theta}$	E^a	A^b	$\sigma^-_{p_r}$	$\sigma^+_{p_r}$	$\sigma^-_{p_\theta}$	$\sigma^+_{p_\theta}$	E^a	A^b
+	+	+	+	∅	0	0	+	+	+	X	J_6	−	+	+	+	T_C	−1
+	+	+	0	X	J_1	0	+	+	0	X	J_7	−	+	+	0	X	J_5
+	+	+	−	∅	0	0	+	+	−	X	J_6	−	+	+	−	T_R	−1
+	+	0	+	∅	0	0	+	0	+	X	J_8	−	+	0	+	T_C	−1
+	+	0	0	∅	0	0	+	0	0	X	J_6	−	+	0	0	T_R	−1
+	+	0	−	∅	0	0	+	0	−	X	J_8	−	+	0	−	T_C	+1
+	+	−	+	∅	0	0	+	−	+	X	J_6	−	+	−	+	T_R	−1
+	+	−	0	X	J_1	0	+	−	0	X	J_7	−	+	−	0	X	J_4
+	+	−	−	∅	0	0	+	−	−	X	J_6	−	+	−	−	T_C	+1
+	0	+	+	X	J_2	0	0	+	+	∅	0	−	0	+	+	X	J_2
+	0	+	0	X	J_3	0	0	+	0	X	J_1	−	0	+	0	X	J_3
+	0	+	−	X	J_2	0	0	+	−	T_R	−1	−	0	+	−	X	J_2
+	0	0	+	X	J_2	0	0	0	+	X	J_9	−	0	0	+	X	J_2
+	0	0	0	X	J_2	0	0	0	0	∅	0	−	0	0	0	X	J_2
+	0	0	−	X	J_2	0	0	0	−	X	J_9	−	0	0	−	X	J_2
+	0	−	+	X	J_2	0	0	−	+	T_R	−1	−	0	−	+	X	J_2
+	0	−	0	X	J_3	0	0	−	0	X	J_1	−	0	−	0	X	J_3
+	0	−	−	X	J_2	0	0	−	−	∅	0	−	0	−	−	X	J_2
+	−	+	+	T_C	+1	0	−	+	+	X	J_6	−	−	+	+	∅	0
+	−	+	0	X	J_4	0	−	+	0	X	J_7	−	−	+	0	X	J_1
+	−	+	−	T_R	−1	0	−	+	−	X	J_6	−	−	+	−	∅	0
+	−	0	+	T_C	+1	0	−	0	+	X	J_8	−	−	0	+	∅	0
+	−	0	0	T_R	−1	0	−	0	0	X	J_6	−	−	0	0	∅	0
+	−	0	−	T_C	−1	0	−	0	−	X	J_8	−	−	0	−	∅	0
+	−	−	+	T_R	−1	0	−	−	+	X	J_6	−	−	−	+	∅	0
+	−	−	0	X	J_5	0	−	−	0	X	J_7	−	−	−	0	X	J_1
+	−	−	−	T_C	−1	0	−	−	−	X	J_6	−	−	−	−	∅	0

[a]Event type: see text for definitions of T_C and T_R; X, ambiguous; ∅, not any type of classified event.
[b]Action type: J_1, store $\sigma^-_{p_\theta}$ in s_θ; J_2, store $\sigma^-_{p_r}$ in s_r; J_3, do both J_1 and J_2; J_4, T_C event with $a_\gamma(T_C)=+1$ followed by J_1; J_5, as J_4 but $a_\gamma(T_C)=-1$; J_6, do lookup with $(s_r, \sigma^+_{p_r}, \sigma^-_{p_\theta}, \sigma^-_{p_\theta})$; J_7, do both J_6 and J_1; J_8, do lookup with $(s_r, \sigma^+_{p_r}, s_\theta, \sigma^+_{p_\theta})$; J_9, do lookup with $(\sigma^-_{p_r}, \sigma^-_{p_r}, s_\theta, \sigma^+_{p_\theta})$.

action J_9 is identical to J_6 but with the roles of p_r and p_θ reversed, and J_8 is the case where both $\sigma^-_{p_r,p_\theta}=0$ require substitution.

The algorithms described for finding T_0, T_C, and T_R events using Tables I and II are implemented easily in the form of lookup tables which can be used to update k_γ after every integration step in an ordinary differential equation routine; in the case of variable step integrators such as that of Bulirsch and Stoer, the lookup tables should only be applied after an accepted integration step. Such an implementation assumes that the time step size of the integrator is not so large as to possibly contain more than one $t_i \in T$.

[1] J. B. Barbour, *The Discovery of Dynamics*, Absolute or Relative Motion? A Study from a Machian Point of View of the Discovery and the Structure of Dynamical Theories, Vol. 1 (Cambridge University Press, New York, 1989).

[2] C. Stoica, Celest. Mech. Dyn. Astron. **84**, 223 (2002).

[3] R. E. Olson, in *Atomic, Molecular and Optical Physics Handbook*, 1st ed., edited by G. W. F. Drake (AIP Press, Woodbury, NY, 1996), Chap. 56, pp. 664–668.

[4] A. Burgess and I. C. Percival, Adv. At. Mol. Phys. **4**, 109 (1968).

[5] E. A. Mason and J. T. Vanderslice, J. Chem. Phys. **31**, 594 (1959).

[6] A. Rapisarda and M. Baldo, Phys. Rev. Lett. **66**, 2581 (1991).

[7] M. A. Karolewski, Surf. Interface Anal. **27**, 114 (1999).

[8] R. Guantes, A. S. Sanz, J. Margalef-Roig, and S. Miret-Artés, Surf. Sci. Rep. **53**, 199 (2004).

[9] R. Smith, M. Jakas, D. Ashworth, B. Oven, M. Bowyer, I. Chakarov, and R. Webb, *Atomic and Ion Collisions in Solids and at Surfaces: Theory, Simulation and Applications* (Cambridge University Press, Cambridge, U.K., 1997).
[10] A. S. Dickinson and D. Richards, Adv. At. Mol. Phys. **18**, 165 (1982).
[11] R. N. Porter and L. M. Raff, in *Dynamics of Molecular Collisions: Part B*, edited by W. H. Miller, Modern Theoretical Chemistry, Vol. 2 (Plenum Press, New York, 1976), Chap. 1, pp. 1–52.
[12] D. G. Truhlar and J. T. Muckerman, in *Atom-Molecule Collision Theory: A Guide for the Experimentalist*, edited by R. B. Bernstein, Physics of Atoms and Molecules (Plenum Press, New York, 1979), Chap. 16, pp. 505–566.
[13] J. D. Sierra, P. A. Enríquez, D. Troya, and M. González, Chem. Phys. Lett. **399**, 527 (2004).
[14] C. Jung, Acta Phys. Pol. B **23**, 177 (1992).
[15] E. Ott and T. Tél, Chaos **3**, 417 (1993).
[16] M. Klein and A. Knauf, *Classical Planar Scattering by Coulombic Potentials*, Lecture Notes in Physics (Series m: Monographs) Vol. 13 (Springer-Verlag, Berlin, 1992).
[17] M. C. Gutzwiller, in *Quantum and Chaos: How Incompatible? Proceedings of the 5th Yukawa International Seminar* (1993), edited by K. Ikeda [Prog. Theor. Phys. Suppl.116, 1 (1994)].
[18] J.-M. Rost, Phys. Rep. **297**, 272 (1998).
[19] L. D. Landau and E. M. Lifshitz, *Mechanics*, 3rd ed., Course of Theoretical Physics, Vol. 1 (Butterworth-Heinemann, Oxford, 1976).
[20] J. V. José and E. J. Saletan, *Classical Dynamics: A Contemporary Approach* (Cambridge University Press, Cambridge, U.K., 1998).
[21] D. G. Babbitt, J. Math. Phys. **12**, 53 (1971).
[22] R. G. Newton, *Scattering Theory of Waves and Particles*, 2nd ed., Texts and Monographs in Physics (Springer-Verlag, New York, 1982).
[23] J. N. Murrell and S. D. Bosanac, *Introduction to the Theory of Atomic and Molecular Collisions* (John Wiley & Sons, Chichester, U.K., 1989).
[24] M. S. Child, *Molecular Collision Theory* (Dover Publications, Mineola, NY, 1996).
[25] H. Pauly, in *Atom-Molecule Collision Theory: A Guide for the Experimentalist* (Ref. [12]), Chap. 4, pp. 111–201.
[26] E. A. Mason, J. Chem. Phys. **26**, 667 (1957).
[27] K. T. Hansen and A. Kohler, Phys. Rev. E **54**, 6214 (1996).
[28] R. J. Cross, Jr., J. Chem. Phys. **46**, 609 (1967).
[29] F. T. Smith, R. P. Marchi, and K. G. Dedrick, Phys. Rev. **150**, 79 (1966).
[30] E. A. Gislason and J. G. Sachs, Chem. Phys. **25**, 155 (1977).
[31] F. E. Budenholzer and E. A. Gislason, J. Chem. Phys. **68**, 4222 (1978).
[32] N. Nešković, B. Perović, and D. Ćirić, Phys. Lett. **96A**, 183 (1983).
[33] P. K. Papachristou, F. K. Diakonos, E. Mavrommatis, and V. Constantoudis, Phys. Rev. E **64**, 016205 (2001).
[34] J. C. Maxwell, Philos. Trans. R. Soc. London **157**, 49 (1867).
[35] S. H. Bauer, Int. J. Chem. Kinet. **37**, 191 (2005).
[36] J. O. Hirschfelder, R. B. Bird, and E. L. Spotz, J. Chem. Phys. **16**, 968 (1948).
[37] *Handbook of Mathematical Functions with Formulas, Graphs and Mathematical Tables*, edited by M. Abramowitz and I. A. Stegun (Dover Publications, New York, 1965).
[38] W. H. Press, S. A. Teukolsky, W. T. Vetterling, and B. P. Flannery, *Numerical Recipes in FORTRAN: The Art of Scientific Computing*, 2nd ed. (Cambridge University Press, New York, 1992).
[39] D. R. Matusek, Ph.D. thesis, Carleton University, Ottawa, Canada, 2003 (unpublished).
[40] K. W. Ford and J. A. Wheeler, Ann. Phys. (N.Y.) **7**, 259 (1959).
[41] A. P. S. de Moura and C. Grebogi, Phys. Rev. E **65**, 035206(R) (2002).